

Pressure- and field-dependent behavior of YbCu₄Au

E. Bauer, E. Gratz, R. Hauser, Le Tuan, A. Galatanu, A. Kottar, H. Michor, W. Perthold, and G. Hilscher
Institut für Experimentalphysik, Technische Universität Wien, A-1040 Wien, Austria

T. Kagayama and G. Oomi

Department of Physics, Kumamoto University, Kumamoto 860, Japan

N. Ichimiya and S. Endo

Research Center for Extreme Materials, Osaka University, Osaka 565, Japan

(Received 11 April 1994)

Temperature- and pressure-dependent measurements of the electrical resistivity $\rho(T, p)$ of the ternary compound YbCu₄Au have been performed. These investigations yield an increase of the antiferromagnetic transition temperature T_N from 0.6 K at ambient pressure up to more than 2 K at 50 kbar. The bulk modulus has been determined ($B_0 \approx 1.4$ Mbar) at room temperature which together with $\partial T_N / \partial p \approx 0.044$ K/kbar derived from $\rho(T, p)$ allows an estimation of the Grüneisen constant $\Omega(T_N) \approx 60$. A study of the field-dependent behavior of the specific heat justifies an antiferromagnetic ground state. In the scope of an empirical model, the Kondo temperature T_K of YbCu₄Au was obtained to be 1.65 K, which is significantly smaller than the energy of the first excited crystal-field level above the ground-state doublet.

I. INTRODUCTION

The series of YbCu₄*M* compounds (*M*=Ag, Au, and Pd), crystallizing in the cubic MgCu₄Sn structure, is known for a variety of interesting properties at low temperatures.¹⁻¹¹ While the Au- and the Pd-based compounds show long range magnetic order with substantially reduced Yb moments below 0.6 K and 0.8 K, respectively, the Ag-based compound exhibits paramagnetism down to lowest temperatures. Owing to the different ground states of these compounds, the observable physical quantities behave noticeably different in a wide temperature range. For example, the temperature-dependent electrical resistivity $\rho(T)$ of YbCu₄Ag is characterized by a behavior which is typical for a Kondo lattice, i.e., $\rho(T) = \rho_0 + AT^2$ at low temperatures with a huge coefficient *A*, a smooth maximum in the vicinity of $T_\rho^{\max} = 100$ K, and a negative logarithmic contribution. It has been shown that this faint maximum cannot be ascribed to crystal-field (CF) splitting, since an enormous pressure dependence has been observed.¹¹ Rather, the maximum at $T = T_\rho^{\max}$ reflects the characteristic temperature of the system, the Kondo temperature T_K , which strongly decreases as the pressure increases. This pressure dependence of T_K , in turn, implies that the coupling constant times the electronic density of states $JN(E_F)$ is lowered. However, since the coefficient *A*,^{3,11} which is proportional to $N(E_F)$,¹² grows with pressure, one has to anticipate that *J* is rapidly enough lowered with pressure to overcome the increase of $N(E_F)$. Such a pressure response appears to be typical for ytterbium compounds, but is in contrast to cerium- and uranium-based systems.¹³ Furthermore, pressure drives YbCu₄Ag from a state at ambient pressure where $T_K > \Delta_{CF}$ (Δ_{CF}

is the overall crystal-field splitting), to $T_K < \Delta_{CF}$ at elevated values of applied pressure. This causes for the former case the crystal-field ground state of the Yb ion to be eightfold degenerate and the Kondo interaction strength to be much larger than the Ruderman-Kittel-Kasuya-Yosida (RKKY) interaction. Contrarily, if T_K is lowered at high pressure, and therefore $T_K < \Delta_{CF}$, the system is dominated by crystal-field splitting, resulting most likely in a doublet as a crystal-field ground state. This crossover can be traced from the scaling behavior of the electrical resistivity, which is valid for small values of applied pressure, but breaks down at pressures beyond 20 kbar.¹¹

The behavior of YbCu₄Au and YbCu₄Pd, however, is quite different from that of YbCu₄Ag. This is due to the fact that Δ_{CF} for the former compounds is much larger than the respective T_K values. Accordingly the crystalline field of cubic symmetry splits the eightfold degenerate ground state of the Yb ion into two doublets and one quartet. Recent inelastic neutron scattering studies⁵ revealed for YbCu₄Au a Γ_7 doublet as the ground state, followed by a Γ_8 quartet, 3.89 meV above it, while Γ_6 is 6.88 meV above the ground-state doublet. A similar level scheme has been concluded for YbCu₄Pd.⁵ Due to the splitting of the ground state, transport properties like the temperature-dependent resistivity or thermodynamical properties like the specific heat are drastically modified by the thermal population of the respective crystal-field levels. Hence, a different overall behavior in comparison to YbCu₄Ag has been found at ambient pressure.¹

The aim of the present investigation was to study the pressure- and field-dependent properties of YbCu₄Au. It has been shown¹ that at ambient pressure $\rho(T)$ of YbCu₄Au exhibits pronounced maxima, as is the case

for YbCu₄Ag. However, we will show that these maxima are of different origin, which follows from noticeable differences of the pressure response. While the resistivity maximum in the Ag-based compound is inferred from the Kondo lattice properties, the high-temperature maximum in the Au-based compound results from the combined interaction of the Kondo effect and crystal-field splitting. The determination of the bulk modulus of YbCu₄Au and the pressure-dependent variation of the antiferromagnetic transition temperature allows the evaluation of a Grüneisen constant. Moreover, we present field-dependent specific heat measurements, which confirm the antiferromagnetic ground state of YbCu₄Au.

II. EXPERIMENTAL DETAILS

Polycrystalline YbCu₄Au samples were prepared from stoichiometric amounts of elements using high-frequency melting under a protective argon atmosphere. Subsequently, a heat treatment at $T = 750^\circ\text{C}$ during 14 days in an argon atmosphere was applied. The phase purity of the samples was proved from x-ray diffraction measurements. The lattice constant a , which has been deduced at room temperature from a Cr $K\alpha$ diffraction pattern, was found to be $a = 7.0503 \text{ \AA}$. This value agrees with that reported previously.^{1,2} The electrical resistivity of bare-shaped samples was measured using a four-probe dc method in the temperature range 1.5 K up to room temperature. Two different methods to generate high pressure were applied: In a range up to 20 kbar a liquid pressure cell with a 4:1 methanol-ethanol mixture as pressure transmitter was used. Beyond 20 kbar, the Bridgman technique with Al₂O₃ anvils and pyrophyllit gaskets was applied. Steatit served as the pressure transmitting medium. The absolute value of the pressure was determined from the superconducting transition of lead.¹⁴

X-ray diffraction experiments under pressure were carried out with monochromated Mo $K\alpha$ radiation from a rotating-anode-type generator (Rigaku, RU 200) and a position sensitive proportional counter. In that case, hydrostatic pressure was generated by a diamond anvil cell using a medium of methanol and ethanol of 4:1 volume ratio. The culet size was 0.7 mm in diameter. Pressure was determined by a ruby fluorescent method.¹⁵

Specific heat measurements on a sample of about 2 g were performed in external magnetic fields up to 9 T and at temperatures from 1.5 K up to 60 K using a modified Nernst-step-heating technique.

III. RESULTS AND DISCUSSION

Figure 1 shows the temperature-dependent electrical resistivity $\rho(T)$ of YbCu₄Au at various values of applied pressure. Well above 50 K, $\rho(T)$ of YbCu₄Au is dominated by a negative logarithmic contribution to the total resistivity, which is attributed to Kondo interaction processes of the conduction electrons with Yb $4f$ moments. In this high-temperature range, $\rho(T)$ of YbCu₄Au can be described by $\rho(T) = a + bT + c\ln(T)$, where the temperature-independent constant a represents the residual resistivity and bT is due to scattering processes of conduction electrons with thermally excited phonons while the term logarithmic in temperature characterizes the Kondo interaction. Results of a least squares fit according to this expression for the resistivity data at ambient pressure are shown in the inset (a) of Fig. 1 as a solid line. Since the coefficient of the logarithmic contribution does not vary well above 50 K, we conclude that scattering of the conduction electrons takes place in the fully degenerate multiplet of the Yb ion with a total angular momentum $j = 7/2$.

Below 50 K, this dependence is modified due to crystal-field splitting, revealing a change of the available scatter-

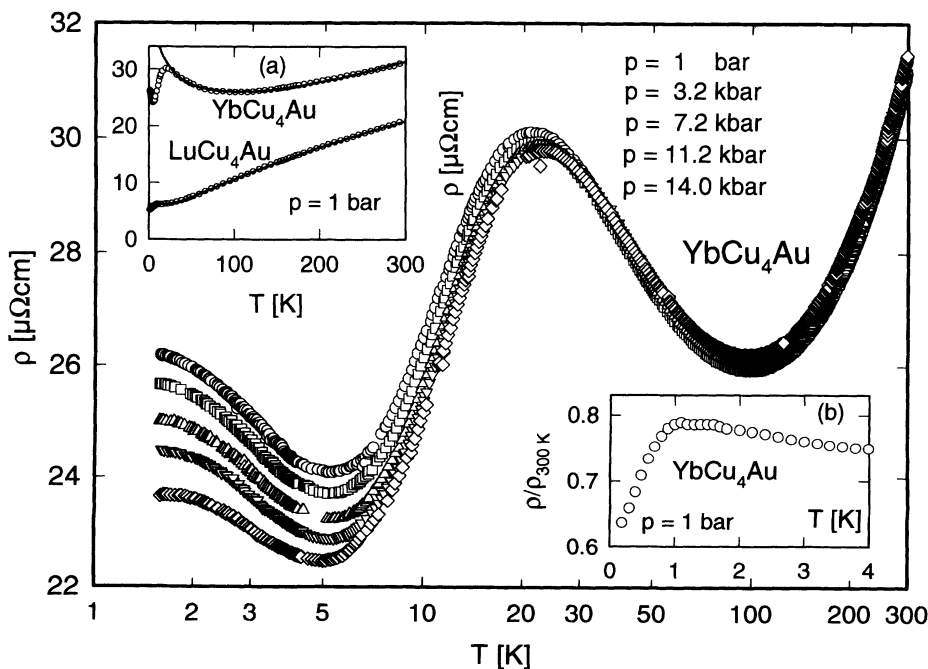


FIG. 1. Temperature-dependent electrical resistivity ρ of YbCu₄Au at various pressures. Inset (a) shows $\rho(T)$ of YbCu₄Au and LuCu₄Au. The solid lines in this inset are least squares fits explained in detail in the text. Inset (b) displays the low-temperature behavior of $\rho(T)$ of YbCu₄Au (Ref. 1).

ing channels. Since at temperatures low enough the excited crystal-field levels are hardly populated, the lower number of scattering channels gives rise to a lowering of the spin-dependent resistivity contribution. For temperatures $2 \text{ K} < T < 4 \text{ K}$, Kondo scattering processes in the crystal-field ground state cause an almost negative logarithmic behavior of the resistivity. Roughly below 1 K the electrical resistivity drops down owing to the onset of long range magnetic order [compare inset (b), Fig. 1 (Ref. 1)].

As the external pressure grows, the absolute resistivity of YbCu_4Au decreases, at least in the lower-temperature range. Simultaneously, a smooth maximum develops in $\rho(T, p)$ in the vicinity of 1.5 K , which is associated with the onset of antiferromagnetic order. At elevated temperatures, the resistivity maximum T_ρ^{max} is shifted to higher temperatures with growing pressure, which most likely follows from an increase of the overall crystal-field splitting Δ_{CF} with rising pressure. Such a behavior may be expected in the scope of the simple point charge model

$$\rho_{\text{ph}}(T) = 4R\Theta_D \left(\frac{T}{\Theta_D} \right)^5 \int_0^{\Theta_D/T} \frac{z^5 dz}{[\exp(z) - 1][1 - \exp(-z)]} - CT^3. \quad (1)$$

Equation (1) takes into account the Debye temperature Θ_D , a temperature-independent constant R , proportional to the electron-phonon interaction strength, and, additionally, the constant C , related to s - d scattering processes. A least squares fit according to Eq. (1) yields rather good agreement with the experimental data. The parameters evaluated are $R = 11 \mu\Omega \text{ cm K}^{-1}$, $\Theta_D = 200 \text{ K}$, and $C = 6.08 \times 10^{-8} \mu\Omega \text{ cm K}^{-3}$. The result of this fit is included in inset (a) of Fig. 1 as a solid line. The application of Eq. (1) seems to be justified, since the isostructural compound LuCu_4In , which is classified as a semimetal²¹ with a carrier density of $n \approx 0.19$ electron/f.u.,²² shows a peak in the electronic density of states below E_F which is originated from Cu p and d states, In p and Lu d states.²¹

Below about 8 K , $\rho(T)$ of LuCu_4Au drops down. This rather uncommon behavior is accompanied with a crossover from paramagnetism above 8 K to diamagnetism below this temperature.²⁰ Since a number of isostructural compounds RCu_4T ($R=\text{Y, Lu}$; $T=\text{Au, Pd, In}$) show similar features,²⁰ we supposed that this low-temperature anomaly is most likely an intrinsic effect of this compound family and attributed it to superconductivity. However, a micrograph analysis shows that a small amount of a not yet identified secondary phase is precipitated which seems to be responsible for the drop of $\rho(T)$ and the diamagnetic signal observed. In this context it is noted that the precipitates of the superconducting secondary phase $\text{YNi}_2\text{B}_2\text{C}$ in YNi_4B exhibit a similar shape as in this system, yielding also an incomplete resistivity drop and diamagnetic signals corresponding to superconductivity fractions up to 60%.²³

In spite of these low-temperature anomalies, LuCu_4Au has been chosen to evaluate $\rho_{\text{mag}}(T)$ of YbCu_4Au . A plot of $\rho_{\text{mag}}(T, p)$ of YbCu_4Au with a logarithmic tempera-

and has been found previously for YbNiSn (Ref. 16) as well as for YbCuAl beyond 100 kbar .¹⁷

To obtain quantitatively the magnetic contribution $\rho_{\text{mag}}(T, p)$ to the total electrical resistivity $\rho(T, p)$, it is necessary to eliminate the residual resistivity ρ_0 , as well as the phonon part $\rho_{\text{ph}}(T)$. Usually, this is done by subtracting the resistivity data of an appropriate isostructural nonmagnetic compound from those of the magnetic compound. Thus, $\rho(T)$ of LuCu_4Au is included in the inset (a) of Fig. 1 for a comparison.

In contrast to the behavior of simple paramagnetic compounds, $\rho(T)$ of LuCu_4Au deviates from the usual linear dependence at elevated temperatures. A description in the scope of the well-known Bloch-Grüneisen formula¹⁸ fails therefore to account for the experimental data. Rather, a modified version of this equation has to be used, which is based on suggestions by Mott and Jones,¹⁹ including scattering processes on a narrow band near the Fermi level E_F . This modified equation can be written as

ture scale is shown in Fig. 2 [$\rho_{\text{mag}}(T) = \rho(\text{YbCu}_4\text{Au}) - \rho(\text{LuCu}_4\text{Au})$]. Note that the pressure related change of $\rho(T)$ of LuCu_4Au has been found to be negligible. $\rho_{\text{mag}}(T, p)$ of YbCu_4Au obtained from this subtraction is characterized by two ranges with an almost logarithmic behavior and a maximum, separating both ranges. This plot again indicates the decrease of the absolute $\rho_{\text{mag}}(T)$ values and the shift of T_ρ^{max} upon increasing pressure. Such a distinct resistivity behavior may be explained in the scope of a model by Cornut and Coqblin,²⁴ which takes into account both the Kondo effect and crystal-field splitting. This model is valid for temperatures above the Kondo temperature, but breaks down below it. Within this model, the magnetic contribution to the electrical resistivity $\rho_{\text{mag}}(T)$ is a sum of the usual spin disorder resistivity and the Kondo ($-\ln T$) term, i.e.,

$$\rho_{\text{mag}}(T) = AN(E_F) \left[\left(\mathcal{V}^2 + \frac{\lambda_n^2 - 1}{\lambda_n(2j+1)} J^2 \right) + J^3 N(E_F) \frac{\lambda_n^2 - 1}{2j+1} \ln \left(\frac{k_B T}{D_n} \right) \right]. \quad (2)$$

Here, A is a constant, \mathcal{V} is the direct interaction strength, λ_n is the effective degeneracy of the occupied $4f$ level, j is the total angular momentum of the magnetic ion, J is the coupling constant, and D_n is a cutoff parameter.

Equation (2) predicts a logarithmic dependence of ρ_{mag} for temperatures much larger or smaller than the temperature of a certain crystal-field level. The logarithmic regime usually observed at low temperatures indicates the Kondo effect in the crystal-field ground state whilst that at high-temperatures is due to the Kondo effect in the fully occupied multiplet of the cerium or ytterbium ion. Moreover, the high-temperature maximum of the

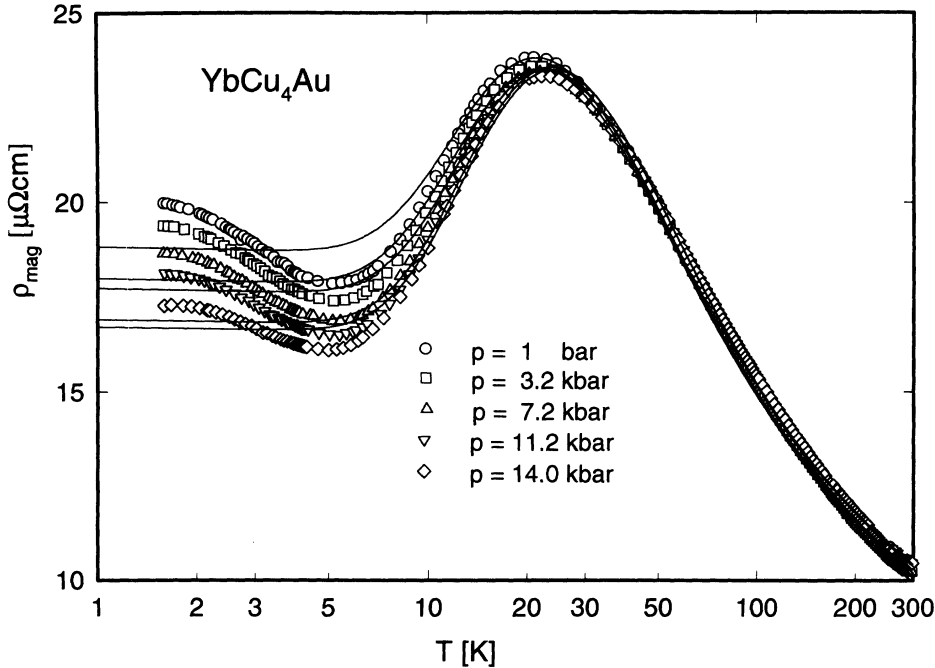


FIG. 2. Temperature-dependent magnetic contribution to the electrical resistivity ρ_{mag} of YbCu₄Au at various pressures plotted in a semilogarithmic representation. The solid lines in this inset are least squares fits explained in detail in the text.

resistivity data coincides roughly with the value of the overall crystal-field splitting Δ_{CF} . A least squares fit according to Eq. (2) reveals satisfactory agreement with the data at elevated temperatures, while deviations occur at lower temperatures.

The decrease of the absolute resistivity values at low temperatures upon pressure indicates according to the first term of Eq. (2) that the product $J^2N(E_F)$ decreases. Previously, it has been shown for Yb compounds that, while J decreases strongly upon pressure, $N(E_F)$ rises. The latter fact was concluded from both the pressure-derived increase of the Sommerfeld value γ observed, e.g., for YbCuAl (Ref. 25) or for Yb₂Cu₉ (Ref. 26) as well as from the increase of A in $\rho = \rho_0 + AT^2$.^{3,11} However, although $N(E_F)$ increases, a much stronger decrease of J has to compensate that rise, and consequently, the product $JN(E_F)$ decreases. By analogy with the aforementioned Yb compounds, we suppose for YbCu₄Au that according to the reduction of $J^2N(E_F)$ also $JN(E_F)$ decreases.

Thus, the lowering of $JN(E_F)$ in YbCu₄Au infers that the initial balance at ambient pressure between the RKKY interaction and the Kondo effect changes. Due to the fact that both RKKY and Kondo interactions depend in a different manner on $JN(E_F)$, the pressure-related decrease of $JN(E_F)$ causes the RKKY interaction to overwhelm the Kondo effect. Accordingly, long range magnetic order is favored and the transition temperature is therefore expected to rise.

In order to demonstrate this unique pressure dependence of ytterbium systems we have studied $\rho(T)$ of YbCu₄Au up to about 70 kbar in the low-temperature region (Fig. 3). The expected pressure-induced increase of T_N can be seen from the shift of the low-temperature resistivity maximum T_{max}^N to higher temperatures, which at ambient pressure appears to be in the proximity of the

magnetic phase transition¹ [compare inset (b) of Fig. 1]. To obtain a resistivity maximum also for smaller values of applied pressure we tried to describe $\rho(T, p)$ in the low-temperature range using a simple polynomial function. Assuming for a first approximation that the maximum of this function depends mainly on pressure, we were able to estimate a value for T_{max}^N below our accessible temperature range. As the position of this maximum rises up to about 2.8 K, we suppose a similar increase of T_N . This pressure-dependent rise of T_{max}^N is shown as inset in Fig. 3. A comparable pressure-driven increase of T_N has been observed for the compound YbNiSn,¹⁶ where T_N rises from about 5.5 K at ambient pressure to 7.6 K roughly at 15 kbar.

Figure 4 shows the relative change of the volume of the unit cell V/V_0 of YbCu₄Au as a function of pressure at room temperature. V/V_0 decreases smoothly with increasing pressure. No anomaly up to 100 kbar is found, indicating that YbCu₄Au does not undergo a pressure-induced phase transition at room temperature. The volume change of YbCu₄Au can be accounted for considering the first order Murnaghan's equation of state²⁷

$$\frac{V_0 - V}{V_0} = 1 - \left(\frac{B_0^*}{B_0} p + 1 \right)^{-\frac{1}{B_0^*}}, \quad (3)$$

where B_0 is the bulk modulus and B_0^* its pressure derivative. The result of a least squares fit gives $B_0 = 1395$ kbar and $B_0^* = 3.5$ and is displayed as a solid line in Fig. 4.

These values can be used to determine a Grüneisen parameter $\Omega(T_i)$ which expresses the volume dependence of various characteristic temperatures (T_i) of the system. From the pressure-dependent variation of T_N (compare inset, Fig. 3) one obtains $\Omega(T_N) = -\partial(\ln T_N)/\partial(\ln V) = (B_0/T_N)(\partial T_N/\partial p)$. Using $\partial T_N/\partial p \approx 0.044$ K/kbar, one arrives finally at $\Omega(T_N) \approx 60$ for YbCu₄Au. Usually,

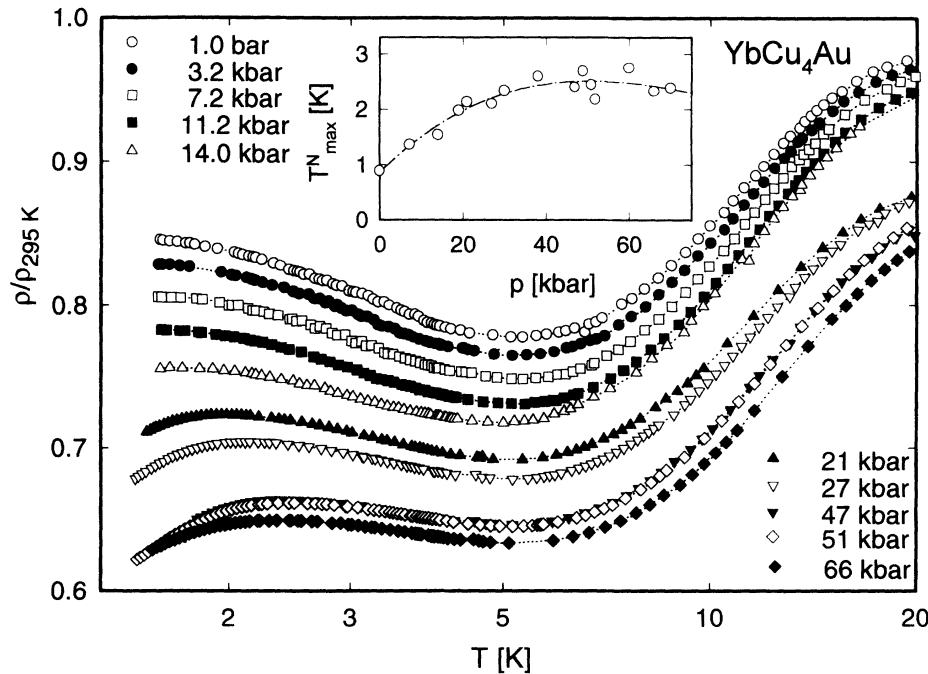


FIG. 3. Electrical resistivity ρ of YbCu_4Au at various pressures in the low-temperature range. The inset shows the pressure dependence of $T_{N_{\text{max}}}^N$ and contains data of different measurements on various specimens of the same batch.

heavy fermion compounds exhibit large values of $\Omega(T_i)$ (of the order of 100) implying that the volume plays an essential role in electronic and magnetic instabilities of such systems.¹³

Figure 5 displays the temperature-dependent specific heat $c(T)$ of YbCu_4Au measured at various values of external magnetic fields. For the purpose of comparison we have included the data of the isostructural reference compound LuCu_4Au , representing the phonon contribution to $c(T)$. The latter compound can be described in a rather limited temperature region (1.5 K–15 K) with a Debye function ($\Theta_D = 225$ K) and a Sommerfeld value γ of about 8 mJ/molK². The former value agrees satisfactorily with Θ_D obtained from the analysis of the resistivity data. The temperature dependence of the specific heat of YbCu_4Au , studied below 1.5 K,¹ is added to this

figure, yielding a remarkably good agreement with the present measurements. The low-temperature data clearly exhibit long range magnetic order below $T_N \approx 0.6$ and coincide with previously reported results of Besnus *et al.*⁷ The data of Rossel *et al.*¹ are shown in more detail as an inset in Fig. 4. The specific heat maximum of YbCu_4Au , which is associated with the magnetic phase transition, is strongly reduced compared to that expected for ordering within a doublet as crystal-field ground state. Moreover, the magnetic entropy below T_N is much smaller than $R \ln 2$. Both facts are attributed to the impact of the Kondo effect, which reduces the magnitude of the magnetic moments involved. The broadening of the phase transition and the high-temperature tail of the specific heat anomaly is referred to short range order effects. An analysis of these data applying an empirical model^{7,28–30}

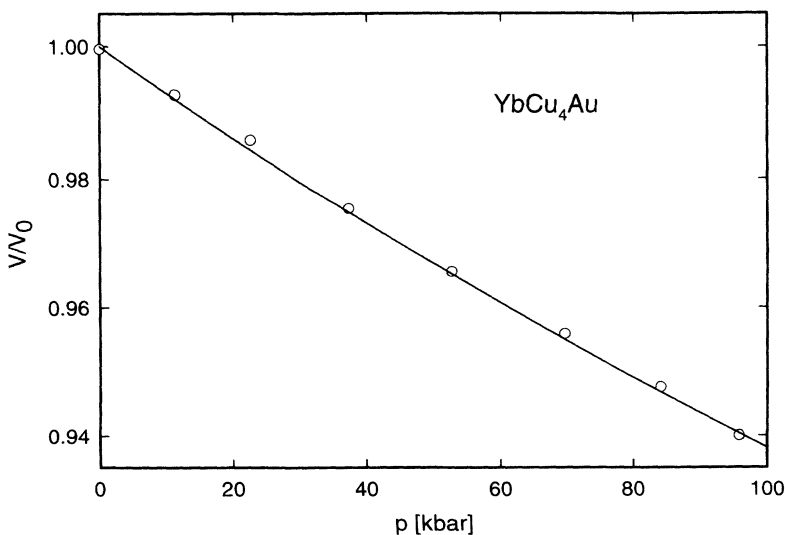


FIG. 4. Relative change of the volume V/V_0 of YbCu_4Au as a function of pressure. The solid line is a least squares fit according to Eq. (3).

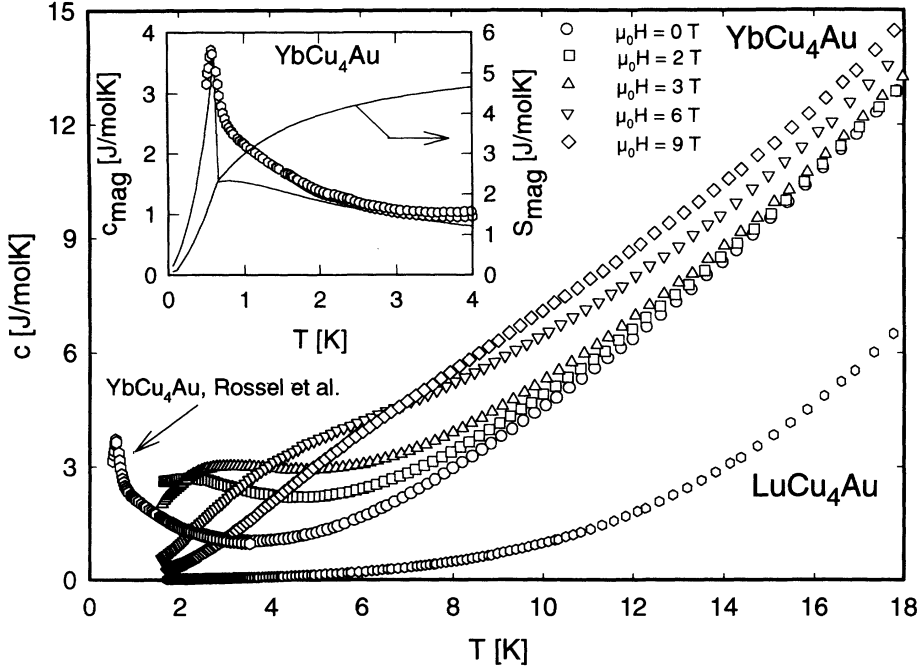


FIG. 5. Temperature-dependent specific heat c of YbCu_4Au for different applied magnetic fields and of LuCu_4Au at zero field. The inset shows $c(T)$ of YbCu_4Au at low temperatures (Ref. 1). The solid line is a fit explained in detail in the text.

allows the determination of both the exchange coupling constant \mathcal{J} and the Kondo temperature T_K . This model is based on the Kondo effect represented in the scope of calculations by Schotte and Schotte³¹ and incorporates magnetic order within a mean field approximation. Both effects together reveal long range magnetic order for $\mathcal{J}/T_K > \pi/2$. Below this value, the Kondo effect is dominating the RKKY interaction and long range order will not be established. Reasonable agreement of the model calculation with the data of Rossel *et al.*,¹ can be found for $\mathcal{J} = 3.4$ K and $T_K = 1.65$ K. The results of these calculations are shown as solid line in the inset of Fig. 4. The values of \mathcal{J} and T_K deduced from this analysis are in agreement with those reported by Besnus *et al.*⁷

On applying magnetic fields, we expect that T_N is suppressed and the degeneracy of the ground-state doublet is lifted by Zeeman splitting in YbCu_4Au . Accordingly the separation between the remaining singlets rises with growing fields yielding a shift of the associated Schottky anomaly to higher temperatures. Related to this Zeeman splitting is an entropy transfer, causing an increase of the heat capacity at somewhat elevated temperatures.

As the predominant contributions to the low-temperature specific heat of YbCu_4Au above T_N originate from the Kondo effect and crystal-field splitting, a high-temperature extrapolation of the specific heat data in a c/T vs T^2 representation does not allow one to determine γ^{HT} in the usual manner. Taking the calculated data (with $\mathcal{J} = 3.4$ K and $T_K = 1.65$ K) as a basis to evaluate the electronic contribution to the specific heat, we obtained a value of more than 2 J/molK² for c/T as the temperature approaches zero. Comparable huge c/T values have been found, e.g., for compounds based on CeCu_6 , when Cu is replaced by Au.³² Such a substitution causes the appearance of long range magnetic order. However, the specific heat jump δc , associated with the magnetic phase transition, is also strongly re-

duced with respect to the expected value in a mean field approximation ($\delta c = 12.5$ J/molK). The distinct specific heat behavior of compounds characterized by low T_K values and long range magnetic order below a few kelvins indicates that just a fraction of the $4f$ moments is involved in ordering. The remaining electrons participate in Kondo scattering processes, thus forming those quasiparticles which exhibit strongly enhanced effective masses.

Figure 6 shows the magnetic contribution to the specific heat c_{mag} plotted as c_{mag}/T vs T for various magnetic fields. As in the case of the resistivity, $c_{\text{mag}}(T)$ of YbCu_4Au is obtained by subtracting the data of the isostructural compound LuCu_4Au , i.e., $c_{\text{mag}}(T) = c(\text{YbCu}_4\text{Au}) - c(\text{LuCu}_4\text{Au})$. The inset of Fig. 6 shows c_{mag} with a logarithmic temperature scale in order to display the low-temperature behavior in more detail. According to this low-temperature behavior it seems likely that the antiferromagnetic order is suppressed with rising external fields and the Schottky anomaly due to the Zeeman splitting of the Γ_7 ground-state doublet is shifted to higher temperatures. The superposition of this low-temperature anomaly with those arising from the thermal population of the Γ_8 quartet and the Γ_6 doublet situated 3.89 meV and 6.88 meV, respectively, causes the shoulderlike feature at lower temperatures and the bell-shaped anomaly at about 20 K. The $c(T, H)$ calculations using the aforementioned CF splitting by Severing *et al.*,⁵ displayed as solid lines in Fig. 6, reproduce quite well the experimental data. Note that the discrepancy between the calculation and the experiment is largest for low fields since for this calculation only the CF splitting was taken into account without considering antiferromagnetic order and the Kondo effect. The latter two have been taken into account for the zero field calculation to determine the parameters \mathcal{J} and T_K in the inset of Fig. 5.

Thus, in the low-temperature and low-field regime

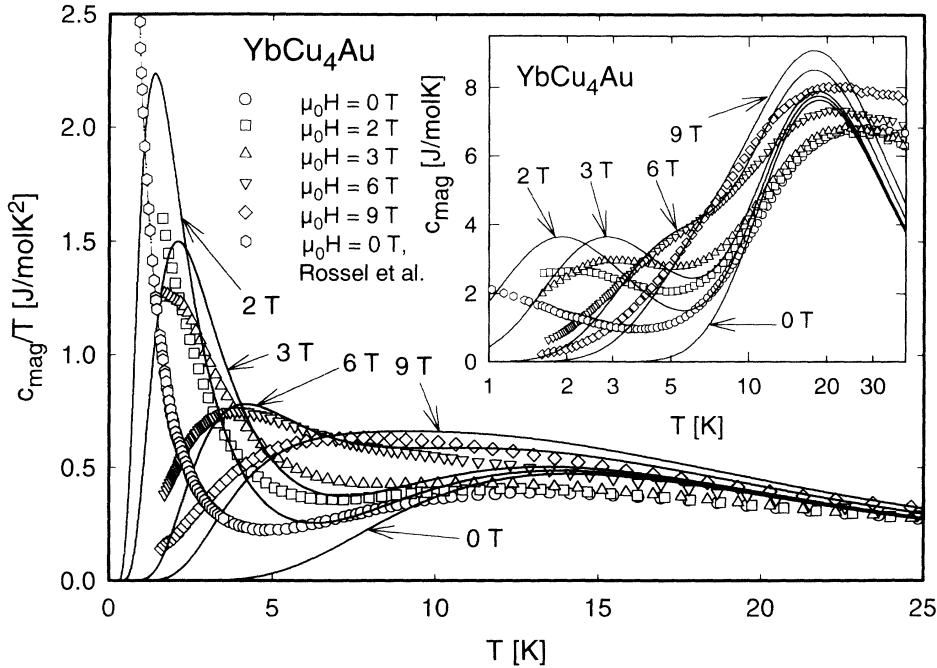


FIG. 6. Magnetic contribution to specific heat c_{mag} of YbCu_4Au plotted as c_{mag}/T vs T for different applied magnetic fields. The solid line represents the behavior due to a Schottky anomaly and Zeeman splitting of the ground-state doublet. The inset shows c_{mag} on a logarithmic temperature scale. Again, the solid lines represent the contribution due to crystal-field splitting and Zeeman splitting of the ground-state doublet.

($H \lesssim 3$ T) regime, the Kondo effect appears to be responsible for the reduced height of the specific heat anomaly observed, since just a fraction of the magnetic entropy is connected with the antiferromagnetic phase transition, while a similar entropy part is spread by the Kondo interaction over a considerable broad temperature range. However, with increasing values of the magnetic field, the agreement between the data and the calculated specific heat behavior is improved, since antiferromagnetic order and the Kondo effect are suppressed and the low-temperature Schottky anomaly moves to higher temperatures, merging that from the excited levels. The discrepancy at higher temperatures between the calculated Schottky anomaly and the measured data is about 10% and may arise also from a different phonon contribution in YbCu_4Au and LuCu_4Au .

IV. SUMMARY

The resistivity and specific heat data obtained for YbCu_4Au clearly indicate that the ground-state properties of this compound follow from a competition between the Kondo effect, the RKKY interaction, and crystal-field effects. Since the exchange constant at ambient pressure and zero magnetic field exceeds the Kondo interaction strength, long range magnetic order appears. However, the transition temperature is reduced from a hypothetical value $T_N^0 \approx 1.7$ K, calculated in the scope of the mean field theory, down to the observed Néel temperature $T_N \approx 0.6$ K. Simultaneously, the magnitude of the magnetic moments involved in the ordering process is reduced by the Kondo effect to 52% of its value, expected for the Γ_7 doublet without the Kondo effect. Both the reduction of the antiferromagnetic transition temperature and the reduction of the magnetic moments in the

crystal-field ground state due to the Kondo effect follow from the empirical model mentioned.^{28,29,7}

Crystal-field splitting dominates the behavior of the electrical resistivity and the specific heat in the paramagnetic temperature range. This is indicated from a pronounced maximum in $\rho_{\text{mag}}(T)$ and from a Schottky contribution to $c_{\text{mag}}(T)$. This behavior is quite different from that of the isostructural compound YbCu_4Ag . The latter compound is dominated by a single temperature scale, namely, the Kondo temperature T_K . The analysis of thermodynamical data in the scope of the Coqblin-Schrieffer model yields a characteristic temperature $T_K \approx 150$ K.^{1,4} The unusual large value of T_K exceeds both RKKY interaction as well as crystal-field splitting. Therefore, the Kondo effect acts in the full $j = 7/2$ state of the Yb ion causing the magnetic moment of Yb to be screened much above the characteristic temperatures of crystal-field splitting and the RKKY interaction, respectively. Theoretically, it has been shown³³ that a large degeneracy of the ground state N enhances the stability of a moment-compensated ground state against a magnetic instability. This follows from a reduction of the critical parameter $|JN(E_F)|_c$ as $O(1/N)$. This critical parameter separates the moment compensated state with $|JN(E_F)| > |JN(E_F)|_c$ from a state with almost stable moments with $|JN(E_F)| < |JN(E_F)|_c$.

The fact that YbCu_4Au at low temperatures appears to be more “magnetic” than YbCu_4Ag is surprising since Au and Ag are considered to be isoelectronic and moreover the lattice parameter of the Ag-based compound is larger than the Au one. Generally, the larger lattice spacing favors the stabilization of magnetism in a band picture. However, since for Yb compounds the $4f^{13}$ state, with $r(4f^{13}) < r(4f^{14})$, is responsible for the magnetic behavior of the system, it is conceivable that the reduced lattice constant is, at least partly, the origin of

long range magnetic order. This conclusion seems to be supported by the increase of the magnetic transition temperature upon increasing pressure and by the crossover of YbCu₄Ag to a behavior with pronounced crystal-field influence and a rather reduced Kondo temperature at high values of applied pressure.¹¹

ACKNOWLEDGMENTS

This work has been supported by the "Austrian Science Foundation" under Project No. P7608-PHY. One of us (E.B.) is indebted to the "Österreichische Forschungsgemeinschaft" for financial support.

-
- ¹ C. Rossel, K.N. Yang, M.B. Maple, Z. Fisk, E. Zirngiebl, and J.D. Thompson, *Phys. Rev. B* **35**, 1914 (1987).
- ² D.T. Adroja, S.K. Malik, B.D. Padalia, and R. Vijayaraghavan, *J. Phys. C* **20**, L307 (1987).
- ³ J.D. Thompson, H.A. Borges, Z. Fisk, S. Horn, R.D. Parks, and G.L. Wells, in *Theoretical and Experimental Aspect of Valence Fluctuations and Heavy Fermions*, edited by L.C. Gupta and S.K. Malik (Plenum, New York, 1987), p. 151.
- ⁴ M.J. Besnus, P. Haen, N. Hamdaoui, A. Herr, and A. Meyer, *Physica B* **163**, 571 (1990).
- ⁵ A. Severing, A.P. Murani, J.D. Thomson, Z. Fisk, and C.K. Loong, *Phys. Rev. B* **41**, 1739 (1990).
- ⁶ H. Nakamura, K. Nakajima, Y. Kitaoka, K. Asayama, K. Yoshimura, and T. Nitta, *Physica B* **171**, 238 (1990).
- ⁷ M.J. Besnus, A. Braghta, N. Hamdaoui, and A. Meyer, *J. Magn. Magn. Mater.* **104 & 107**, 1385 (1992).
- ⁸ G. Polatsek and P. Bonville, *Z. Phys. B* **88**, 189 (1992).
- ⁹ P. Schlottmann, *J. Appl. Phys.* **73**, 5412 (1993).
- ¹⁰ P. Waibel, M. Grioni, D. Malterre, B. Dardel, Y. Baer, and M.J. Besnus, *Z. Phys. B* **91**, 341 (1993).
- ¹¹ E. Bauer, R. Hauser, E. Gratz, K. Payer, G. Oomi, and T. Kagayama, *Phys. Rev. B* **48**, 15873 (1993).
- ¹² W.G. Barber, *Proc. R. Soc. London* **258**, 383 (1937).
- ¹³ J.D. Thompson, in *Frontiers in Solid State Sciences*, edited by L.C. Gupta and M.S. Multani (World Scientific, London, 1993), Vol. 2, p. 107.
- ¹⁴ A. Eiling and J. Schilling, *J. Phys. F* **11**, 623 (1981).
- ¹⁵ R.A. Forman, G.J. Piermarini, J.D. Barnett, and S. Block, *Science* **176**, 284 (1972).
- ¹⁶ G. Sparn and J.D. Thompson, *J. Alloys Compounds* **181**, 197 (1992).
- ¹⁷ J.M. Mignot and J. Wittig, in *Physics and Solids under High Pressure*, edited by J.S. Schilling and R.N. Shelton (North-Holland, Amsterdam, 1981), p. 311.
- ¹⁸ G. Grimvall, *The Electron-Phonon Interaction in Metals* (North-Holland, Amsterdam, 1981).
- ¹⁹ N.F. Mott and H. Jones, *The Theory of the Properties of Metals and Alloys* (Oxford University Press, London, 1958).
- ²⁰ E. Bauer, M. Forsthuber, R. Hauser, G. Hilscher, T. Holubar, R. Resel, and G. Schaudy, *Physica B* **194-196**, 1163 (1994).
- ²¹ K. Takegahara and T. Kasuya, *J. Phys. Soc. Jpn.* **59**, 3299 (1990).
- ²² F. Marabelli and E. Bauer, *J. Appl. Phys.* **73**, 5418 (1993).
- ²³ N.M. Hong, H. Michor, M. Vybornov, T. Holubar, P. Hundegger, W. Perthold, G. Hilscher, and P. Rogl, *Physica C* **227**, 85 (1994).
- ²⁴ D. Cornut and B. Coqblin, *Phys. Rev. B* **5**, 4541 (1972).
- ²⁵ A. Bleckwedel, A. Eichler, and R. Pott, *Physica B* **107**, 93 (1981).
- ²⁶ A. Amato, R.A. Fisher, N.E. Phillips, D. Jaccard, and E. Walker, *Physica B* **165-166**, 389 (1990).
- ²⁷ F.D. Murnaghan, *Finite Deformation of an Elastic Solid* (Dover, New York, 1951), p. 68.
- ²⁸ C.D. Bredl, F. Steglich, and K.D. Schotte, *Z. Phys. B* **29**, 327 (1978).
- ²⁹ A. Braghta, Ph.D. thesis, University of Strasbourg, 1989.
- ³⁰ E. Bauer, G. Schaudy, G. Hilscher, L. Keller, P. Fischer, and A. Dönni, *Z. Phys. B* **94**, 359 (1994).
- ³¹ K.D. Schotte and U. Schotte, *Phys. Lett.* **55A**, 38 (1975).
- ³² H.G. Schlager, A. Schröder, M. Welsch, and H.v. Löhneysen, *J. Low Temp. Phys.* **90**, 181 (1993).
- ³³ P. Coleman, *Phys. Rev. B* **28**, 5255 (1983).